Biophysical characterization of hydrogel-core, lipid-shell nanoparticles (nanolipogels) for HIV chemoprophylaxis

Reena Mahadevan

A thesis submitted in partial fulfillment of the requirements for the degree of:

Master of Science

University of Washington

2013

Committee:

Dr. Kim Woodrow

Dr. Deok-Ho Kim

Program Authorized to Offer Degree:

Department of Bioengineering

University of Washington

Abstract

Biophysical characterization of hydrogel-core, lipid-shell nanoparticles (nanolipogels) for HIV chemoprophylaxis

Reena Mahadevan

Chair of the Supervisory Committee:

Dr. Kim Woodrow

Bioengineering

Nanoparticles are emerging as versatile vehicles for drug delivery, providing targeting, protection, and controlled-release capabilities to encapsulated cargo. Polymeric nanoparticles made from poly(lactide-co-glycolide) (PLGA) are biodegradable, exhibit tunable drug release, and have encapsulated a wide variety of biological agents. However, PLGA nanoparticles are relatively inefficient at encapsulating small-molecule hydrophilic drugs. Liposomes encapsulate greater amounts of hydrophilic agents and demonstrate good cellular affinity; however, they lack controlled-release functionality. Hydrogel-core lipid-shell nanoparticles, or nanolipogels, combine the controlled-release capability of polymeric nanocarriers with the hydrophilic and cellular affinity of liposomes into a single drug delivery vehicle. This study establishes a facile, reproducible synthetic protocol for nanolipogels and evaluates hydrogel swelling as a mechanism for release of the small hydrophilic antiretroviral azidothymidine from nanolipogels.

Specific aims

Nanoparticles are versatile carriers for delivery of a wide variety of biological agents. These systems protect cargo against in vivo degradation and are readily functionalized for specific targeting and controlled release. The release kinetics of small-molecule drugs can be readily modified by varying nanoparticle parameters such as size, charge, and composition [1]. Choice of biomaterial for the nanoparticle depends on and limits the biological agents that can be encapsulated. For example, poly(lactic-co-glycolic) acid (PLGA), a nontoxic, biodegradable, FDA-approved polymer commonly used in nanoparticle synthesis, is effective at encapsulating a wide variety of hydrophobic agents both singly and in combination and at exhibiting controlled release of these agents [2]. However, PLGA nanoparticles have limited efficiency in encapsulating highly hydrophilic small molecule drugs. Liposomes, which contain an aqueous core, have shown high encapsulation efficiency of azidothymidine [3] and tenofovir [4], but demonstrate low drug loading overall and limited controlled-release capabilities. An ideal nanoparticle-based drug delivery system would combine the aqueous affinity of liposomes with the controlled-release capabilities of polymeric nanocarriers.

Hydrogel-core lipid-shell nanoparticles, or nanolipogels, are a structure of particular interest as they combine properties of liposomes and polymeric nanoparticle systems. The aqueous hydrogel core allows for encapsulation of hydrophilic components. Bulk and particulate hydrogel systems have successfully encapsulated and released whole cells [2], small proteins [1], and large proteins [5] as well as small-molecule hydrophilic drugs [4] over 24-hour time frames. The lipid shell can provide an additional barrier to burst release as well as be used for encapsulating hydrophobic drugs, facilitating single-vehicle combination therapy within one carrier. I hypothesize that loading small-molecule antiretroviral drugs within nanolipogels with varying ratios of monomer to crosslinker in the hydrogel core will result in varying rates and extents of swelling within the hydrogel, resulting in tunable controlled release of hydrophilic small molecule drugs.

Aim 1: Establish reproducible methods for synthesis and characterization of nanolipogels and validate hydrogel-core, lipid-shell architecture.

- Development of synthetic protocol for nanolipogels using UV gelation within liposome reactor; evaluate for ease and reproducibility
- Characterization of size, PDI, and zeta potential of nanoparticles using DLS; evaluate for consistency
- Conformation of hydrogel-core lipid-shell structure using detergent solubilization and TEM

Aim 2: Evaluate differences in hydrogel swelling as a mechanism for modulating drug release.

- Equilibrium water content testing on bulk hydrogels with low and high crosslinker concentrations to determine differences in swelling
- Rheological studies on bulk hydrogels to determine differences in mechanical properties based on monomer and crosslinker concentration
- Determination of drug loading/ release profiles on a panel of HIV drugs alone and in combination using HPLC

Table of Contents

List of Tables

List of Figures

Chapter 1

Chapter 2

CHAPTER 1: SYNTHESIS OF HYDROGEL-CORE, LIPID-SHELL NANOPARTICLES (NANOLIPOGELS)

Introduction

Nanoparticles are emerging as highly effective and versatile vehicles for drug delivery. Though the most commonly studied nanoparticles are spherical carriers between 100-1000 nm in diameter, they can also be pyramidal, cylindrical, or cubical, among other shapes [6]. A wide variety of materials can be used to synthesize nanoparticles, including polymers, metals, semiconductors, lipids, peptides, and nucleic acids [7]–[11]. This variety in material compositions allows for the encapsulation and release of a wide range of biological agents. The high surface-area-to-volume ratio of nanoparticles facilitates the creation of unique surface chemistries and incorporation of antibodies or ligands for targeted delivery of drugs or other cargo in vivo. Encapsulating drugs within targeted nanoparticles increases availability at the target site, prevents premature degradation, and increases circulation time [10]. Modulation of nanoparticle size and composition can produce controlled release of encapsulated drug, increasing overall bioavailability and efficacy. Two types of nanoparticles particularly relevant to drug delivery are polymeric nanoparticles made from lactic/glycolic acid and liposomes.

Polymeric nanoparticles made from poly(lactic acid) (PLA), poly(D,L-glycolide) (PLG), and poly(lactide-co-glycolide) (PLGA) have been widely studied as drug delivery vehicles [12]. In particular, PLGA nanoparticles are highly efficient at encapsulating small-molecule hydrophobic drugs, such as paclitaxel and doxorubicin [2], [13]. Of particular interest is the success of PLGA nanoparticles at encapsulating the hydrophobic antiretrovirals (ARVs) efavirenz and saquinavir, both used in the treatment of human immunodeficiency virus (HIV) [14]. PLGA nanoparticle synthesis most commonly involves a form of water and oil emulsion [2] PLGA nanoparticles

exhibit controlled release of encapsulated drug, and the rate and degree of release can be tuned for each specific drug through variation of the PLA/PLG ratio within the polymeric nanoparticle. Drug release mechanisms from PLGA nanoparticles include diffusion from intact particles, the rate of which can be modulated by controlling particle porosity via particle composition, and biodegradation of PLGA, the rate of which can be modulated by changing the PLA/PLG ratio. Several PLGA nanoparticle-drug formulations have been FDA-approved due to the nontoxicity and biocompatibility of PLGA [15]. Limitations of PLGA nanoparticles include their relative hydrophobicity, resulting in very limited encapsulation of hydrophilic agents. Efforts within the Woodrow lab to encapsulate the hydrophilic ARVs azidothymidine (AZT) and tenofovir (TFV) within PLGA nanoparticles have proven ineffective Given the many advantages of PLGA nanoparticles, significant efforts have been made to increase their hydrophilic capacity, including the development of a self-healing PLGA formulation and the use of trapping agents such as aluminum hydroxide [16], [17]. These strategies have proved appropriate and effective for hydrophilic proteins, but are not useful for small-molecule hydrophilic drugs that, due to their small size, may not be effectively trapped within the nanoparticle by these mechanisms.

In contrast to polymeric nanoparticles, liposomes consisting of a spherical lipid vesicle with an aqueous core allow for more efficient encapsulation of hydrophilic cargo. Liposomes have been studied as drug delivery vehicles to a similar extent as polymeric nanoparticles. Their simple structure allows for facile synthesis, and variations in lipid composition allow for a wide range of surface chemistries, charges, and rigidities for different applications. As liposomes possess both a lipid phase and an aqueous phase, they have been shown to successfully encapsulate a range of hydrophilic and hydrophobic biological agents. Doxorubicin and paclitaxel have both been encapsulated within the lipid bilayer of liposomes [18], [19], and AZT and TFV have been

encapsulated within the aqueous core [3], [4]. This biphasic structure presents the possibility of combination delivery of hydrophobic and hydrophilic agents within the same nanoparticle. The lipid bilayer can hold cell membrane proteins, targeting ligands, and antibodies in their native conformations for targeted drug delivery. Furthermore, liposomes of many different compositions are easily trafficked into cells, leading to good biodistribution of encapsulated drug. Mechanisms of drug release from liposomes include diffusion across the lipid bilayer, cell membrane fusion, and endocytosis and degradation by cells. Liposome synthesis can occur by a number of well-characterized protocols, including bath sonication of aqueous lipid vesicle solutions [3], extrusion [19], and detergent solubilization and removal [20]. Limitations of liposomes include the lack of controlled-release functionality possessed by polymeric nanoparticles. As drugs encapsulated within liposomes have only to cross over a single lipid bilayer (membrane) as opposed to diffusing through a polymer mesh, liposomes often exhibit burst release of encapsulated drug. This effort can be somewhat moderated by changing lipid composition, but liposomes alone do not reach the full functionality and flexibility in controlled release exhibited by polymeric nanoparticles. As compared to some compositions of polymeric nanoparticles, liposomes have a relatively short circulation lifetime and are degraded in vivo as readily as they are taken up into cells.

Hydrogel-core lipid-shell nanoparticles, or nanolipogels (NLGs), combine the controlled-release functionality of polymeric nanoparticles with the hydrophobic/hydrophilic encapsulation ability and cell affinity of liposomes. These characteristics make NLGs an ideal vehicle for encapsulation and controlled release of small-molecule antiretrovirals used in treatment of HIV. A wide variety of biological agents have been encapsulated and released from NLGs, including proteins [5] and hydrophilic [21], [22] and hydrophobic [23], [24] small-molecule drugs

encapsulated agents include viable whole cells [25], cytokines [22], proteins [5], [22], and small-molecule drugs [24]. NLGs have also been used to encapsulate and deliver combinations of small-molecule hydrophobic drugs and hydrophilic proteins [22]. These studies provide the basis for the formulation of nanolipogels as carriers for small-molecule hydrophilic antiretrovirals.

While NLG-based drug delivery systems are used with increasing frequency in literature, no single method has been established for facile, reproducible NLG synthesis. Most existing methods are similar to the UV gelation within liposome reactors pioneered by Kazakov et al. Briefly, this method involves rehydrating a dry lipid film with hydrogel constituents in solution solution to form multilamellar vesicles (MLVs), which are then reduced to unilamellar vesicles (ULVs) and polymerized under UV light to form hydrogel cores surrounded by lipid bilayers, or NLGs [26]. Existing methods differ most commonly at two key steps in this process: reduction of MLVs to ULVs and removal of unencapsulated hydrogel constituents. In this study, we attempt to determine the best way for modifying these two steps in order to maximize reproducibility of NLGs during synthesis. Establishing a reliable and reproducible method for NLG synthesis will ensure a working population of NLGs within acceptable design parameters for further studies.

Materials and methods

Materials

Egg phosphatidylcholine (EPC); 1,2-dioleoyl-*sn*-glycero-3-phospho-(1'-rac-glycerol) (DOPG); and all needle extruder components were purchased in chloroform from Avanti Polar Lipids. Acrylamide (AAm) monomer, methylene-bis-acrylamide (MBA) crosslinker, and diethoxyacetophenone (DEAP) photonitiator were purchased in aqueous solution from Sigma-Aldrich. Azidothymidine (AZT), a nucleoside reverse transcriptase inhibitor used here as a model small-molecule hydrophilic drug, was purchased from Sigma-Aldrich. Maraviroc (MVC), an entry inhibitor used here as a model small-molecule hydrophobic drug, was purchased from Pfizer. Water used in buffer solution was purified using a Milli-Q purification system (Millipore Corporation).

NLG synthesis

NLGs were synthesized by extending standard liposome synthesis via the methods established by Kazakov, Patton, and Schillemans previously. EPC and DOPG in chloroform at a ratio of 9:1 were placed in a round-bottomed flask, which was attached to a rotary evaporator (Buchi, Flawil, Switzerland) rotating at 120 rpm over a 37° C water bath until all chloroform evaporated, forming a dry lipid film. AAm and MBA at varying concentrations (see Table 1) and DEAP at 2.17 µl/ml were dissolved in 0.1 M citrate buffer. The dry lipid film was then rehydrated with the buffer solution via gentle handshaking and vortexing, forming multilamellar vesicles encapsulating hydrogel constituents. The multilamellar vesicles were reduced to ULVs ~200 nm in diameter via 11 passes through a hand-held needle extruder (Avanti Polar Lipids) using a 0.2 µm polycarbonate membrane. Ascorbic acid at 150 mg/ml was dissolved into the vesicle solution to prevent external polymerization. The ULVs were then polymerized under UV light for 25

minutes, forming the hydrogel-core lipid-shell NLGs. The NLGs were filtered sequentially through 0.45 μm and 0.22 μm membranes to remove externally polymerized material, and then centrifuged to pellet at 14,000g for 10 min. The supernatant was removed and the pelleted NLGs were resuspended in 50 mM Tris-HCl buffer and filtered again through a 0.22 μm membrane.

Physical characterization by dynamic light scattering (DLS) and transmission electron microscopy (TEM)

Size and polydispersity of NLGs were measured using DLS with a Malvern Zetasizer (Malvern Instruments, Malvern, UK). NLGs were diluted 10x in citrate buffer prior to DLS measurement. To confirm the hydrogel-core lipid-shell structure, the nanolipogels were stripped of their lipid bilayers via addition of 10-100 mM Triton-X 100 prior to DLS measurement.

The hydrogel-core lipid-shell morphology of NLGs was further confirmed with TEM. NLGs were applied to a freshly discharged, carbon coated 400 mesh copper grid. Excess sample was blotted off, washed with water, and stained twice with a 0.75% w/w solution of uranyl formate. The preparations were viewed on a transmission electron microscope (FEI, Morgagni) operated at an acceleration voltage of 100kV. Images were recorded on a bottom mount Gatan slow scan charge coupled device (CCD) at a nominal magnification of 25,000x at the specimen level.

Results and Discussion

The basic strategy for UV-induced gelation within liposome reactors, as developed by Kazakov et al., involves rehydrating a dry lipid film with hydrogel constituents and photoinitiator in buffer to form multilamellar vesicles (MLVs) encapsulating hydrogel constituents, reducing the MLVs to unilamellar vesicles (ULVs), and exposing the ULVs to UV light in order to induce polymerization of the hydrogel core, forming the NLG (Figure 2). Hydrophobic drugs are incorporated into the lipid film prior to drying and hydrophilic drugs are added to the rehydration buffer along with hydrogel constituents. Expected parameters for the NLG are a diameter of ~200 nm, a polydispersity index (PDI) of ~0.2 indicating an acceptably monodisperse nanoparticle population, and a hydrogel-core lipid-shell morphology. Size and PDI are evaluated using DLS, and the NLG morphology is confirmed using a combination of DLS after detergent solubilization and cryo-TEM, as detailed in the Methods. These parameters along with their methods of evaluation are summarized in Table 1.Two steps of the NLG synthetic process required modification and optimization during development of the final protocol, as the methods for these steps failed in our hands to produce NLGs within the expected parameters. These two steps were reducing MLVs to ULVs and removing unencapsulated hydrogel constituents and drug.

Reducing MLVs to ULVs: Replacing bath sonication with extrusion improves ULV size control and PDI

Kazakov uses bath sonication to reduce MLVs to ULVs encapsulating hydrogel constituents [26], a strategy which in our hands resulted in a highly polydisperse particle population. Though Kazakov et al. reported good control over ULV size dependent on sonication power and duration, bath sonication allowed us little control over resultant ULV size. Figure 3 shows three

populations of MLVs bath sonicated for different lengths of time. While some time-dependent control over ULV size was apparent, the resulting ULV populations exhibited PDIs > 0.3, indicating an unacceptably polydisperse particle population. Furthermore, bath sonication produced multiple extraneous particle populations both smaller and larger than the target size. Given the failure of the bath sonicator to produce an acceptably monodisperse particle population with its fixed power, an alternate method was needed to produce ULVs from MLVs.

Following the methods of Patton et al., we replaced bath sonication with needle extrusion through a polycarbonate membrane with 200 nm pores [5]. We hypothesized that forcing the MLV solution through a 200 nm filter would allow us better and more direct size control (i.e. ULVs ~200 nm in diameter) than the more indirect method of sonication, with a corresponding decrease in PDI. We found that needle extrusion did indeed result in a monodisperse ULV population with a diameter ~200 nm and a PDI < 0.2. (Figure 4) Extrusion resulted in consistently good size control of the final ULV population with some pass number-dependent variation in PDI, but 11 passes through the polycarbonate membrane was sufficient to produce a monodisperse population. Given the reproducible production of a ULV population of appropriate size and PDI, we established needle extrusion as our preferred method for reducing MLVs to ULVs in our final protocol.

Removal of unencapsulated hydrogel constituents and drug: Ascorbic acid followed by filtration and centrifugation prevents external polymerization while still producing NLGs

Removing or otherwise inactivating hydrogel constituents unencapsulated by ULVs prior to polymerization prevents external polymerization, ensuring the formation of NLGs in solution rather than a hydrogel slab with incorporated NLGs. In addition, removing unencapsulated drug either before or after polymerization ensures that drug release studies from NLGs are not

confounded by the presence of free drug in the NLG solution. The original NLG synthesis protocol established by Kazakov et al. does not include drug encapsulation, as this work was focused solely on the synthesis and characterization of NLGs. Kazakov therefore has no method for removal of unencapsulated drug, but prevents external polymerization through dilution of the ULV solution 20-25x in buffer prior to polymerization. This group reports that dilution prevents external polymerization and results in polymerized NLGs with confirmation of the hydrogel-core lipid-shell structure via detergent solubilization of the lipid layer followed by DLS examination. Solubilization of empty liposomes (LPs) or ULVs with the detergent Triton-X at 10-100 mM produces mixed detergent-lipid micelles 9-11 nm in diameter, yielding a single peak on DLS. Solubilization of the lipid bilayer of NLGs should yield a bare hydrogel nanoparticle population at around 200 nm in addition to the mixed-micelle population, yielding two peaks on DLS and validating the existence of the polymerized hydrogel core. In our hands, dilution of ULVs prior to polymerization prevented external polymerization, but the resulting NLGs could not be validated for hydrogel-core lipid-shell morphology using detergent solubilization and DLS. Only the mixed micelle peak was visible. We theorized that dilution of ULVs was creating sink conditions for the encapsulated hydrogel constituents and driving them out of the ULVs before the hydrogel core could polymerize, leaving essentially empty LPs in place of NLGs. Furthermore, dilution does not remove free drug from the external NLG solution, leaving the risk of confounding NLG drug release studies. The cumulative results of these studies led us to explore other strategies of removing both unencapsulated hydrogel constituents and unencapsulated drug.

We first replaced the dilution step with ultracentrifugation of ULVs after extrusion to remove both unencapsulated hydrogel constituents and free drug prior to polymerization. This strategy

was adopted with the theory that pelleting the ULVs would leave unencapsulated excipients and drug in the supernatant. Since ULVs are comparable to LPs in terms of mass and density, they do not pellet at conventional centrifugation speeds, requiring the use of ultracentrifugation. While this strategy was again successful in preventing external polymerization, the NLGs did not show evidence of polymerized hydrogel cores on DLS (Figure 5), indicating that few or none of them were polymerizing under UV irradiation. We theorized that the forces involved in the ultracentrifugation process drove encapsulated hydrogel constituents out of the ULVs, similar to how the concentration gradient in diluted ULVs may have driven out encapsulated hydrogel constituents. Though ultracentrifugation was successful at pelleting the ULVs, the polymerization failure indicated that this was not a viable strategy for removing unencapsulated hydrogel constituents or free drug.

In order to maximize the population of polymerized NLGs, we amended our strategy to replace ultracentrifugation with the addition of ascorbic acid at 150 mg/ml to the ULVs prior to UV irradiation, as described by Schillemans et al. [20] Photoinitiated polymerization of polyacrylamide relies on free radical generation from the photoinitiator under UV irradiation, catalyzing the covalent crosslinking of the AAm monomers and MBA. Ascorbic acid in the ULV solution acts as a free-radical scavenger, preventing external polymerization of unencapsulated AAm and MBA. Amending the lipid film formulation to include 10% DOPG instead of pure EPC confers a slight negative charge to the ULVs, preventing the negatively-charged ascorbic acid from crossing the lipid bilayers into the core. This allows for uninhibited polymerization of the hydrogel cores. To eliminate any trace external polymerization that may occur during UV irradiation, we filtered polymerized NLGs sequentially through 0.45 µm and 0.22 µm membranes using syringes. This strategy prevented external polymerization and resulted for the

first time in positive confirmation of the hydrogel-core lipid-shell structure by DLS. Detergent-solubilized NLGs displayed both a mixed-micelle and a bare hydrogel nanoparticle population on DLS (Figure 6), confirming the existence of the hydrogel core. NLGs synthesized using this method pelleted under conventional centrifugation at 14,000 rpm, allowing for removal of free drug and unincorporated hydrogel material after polymerization and filtration. This behavior was most likely due to the presence of a denser polymerized hydrogel core as compared to the aqueous cores of LPs and ULVs. LPs and ULVs did not pellet at 14,000 rpm, indicating that the existence of the pellet is a further validation for NLG polymerization. Cryo-TEM images of LPs, ULVs, and NLGs reveal clear differences in structure between these three nanoparticle populations. While all three are ~200 nm in diameter and share a spherical morphology, the LPs and ULVs appear as smooth flattened vesicles while the NLGs appear as flattened vesicles deformed around a solid core (Figure 8). This final check confirms the hydrogel-core lipid-shell morphology and validates the use of ascorbic acid pre-polymerization followed by filtration and centrifugation as a strategy for NLG synthesis.

Final protocol results in monodisperse NLGs ~200 nm in diameter

The final protocol results in reproducible synthesis of hydrogel-core, lipid-shell NLGs (Figure 1). Briefly, a dry lipid film containing hydrophobic drug is rehydrated with hydrogel constituents (monomer, crosslinker, photoinitiator) and hydrophilic drug in buffer, forming MLVs. MLVs are reduced to monodisperse ULVs via needle extrusion. Ascorbic acid is added to the ULV solution to prevent external polymerization. The ULVs are then polymerized via UV irradiation to form NLGs. Unencapsulated excipients and free drug are removed by filtration followed by centrifugation, forming the final NLG population. As Kazakov's original method of bath sonication did not result in a monodisperse ULV population in our hands, we replaced this step

with needle extrusion for greater size control and lower PDI. When Kazakov's method of dilution to prevent external polymerization failed to produce NLGs in our hands (and in other groups' hands as well [20]) due to a possible concentration gradient, we replaced this with ascorbic acid addition pre-polymerization followed by filtration and centrifugation post-polymerization, resulting in confirmed NLG synthesis. Data on NLGs synthesized using the final protocol showing these parameters met is shown in Table 2.

Conclusions

We have developed a facile, reproducible synthetic protocol for monodisperse NLGs ~200 nm in diameter (Figure 7). Previously published protocols for NLG synthesis varied greatly in methodology, particularly in reducing MLVs to ULVs and removing unencapsulated hydrogel constituents and free drug. Many of these protocols failed in our hands, indicating the lack of a unifying paradigm for NLG synthesis of the kind that exists for PLGA nanoparticle or liposome synthesis. Our goal in this study was to develop a protocol that combined the most effective methodology of previously published protocols such that the final protocol would be easily reproducible both by us and by any lab similarly equipped to ours with no failures at the aforementioned synthetic steps. We have established that the size and PDI of the NLGs fall within acceptable parameters using DLS, and we have confirmed the hydrogel-core lipid-shell morphology of the NLGs using detergent solubilization DLS and cryo-TEM imaging. The primary remaining challenge in NLG synthesis is removal of UV irradiation as a means for hydrogel core polymerization. UV irradiation limits potential encapsulated agents in NLGs to non-UV sensitive materials, preventing the encapsulation of some proteins, nucleic acids, and similar biological compounds. Furthermore, use of UV irradiation makes encapsulation of fluorescent dyes for cellular tracking studies of NLGs impossible, as photobleaching occurs. The use of a different polymerization initiator may solve this problem, but preventing polymerization until the ULVs are formed and the external hydrogel components removed remains a challenge. Nevertheless, the NLGs produced by our final protocol are suitable for the encapsulation and release of a wide variety of small-molecule drugs.

References

[1] M. Hamidi, A. Azadi, and P. Rafiei, "Hydrogel nanoparticles in drug delivery," *Adv. Drug Deliv. Rev.*, vol. 60, no. 15, pp. 1638–1649, Dec. 2008.

[2] F. Danhier, E. Ansorena, J. M. Silva, R. Coco, A. Le Breton, and V. Préat, "PLGA-based nanoparticles: An overview of biomedical applications," *J. Controlled Release*, vol. 161, no. 2, pp. 505–522, Jul. 2012.

[3] N. C. Phillips and C. Tsoukas, "Liposomal encapsulation of azidothymidine results in decreased hematopoietic toxicity and enhanced activity against murine acquired immunodeficiency syndrome," *Blood*, vol. 79, no. 5, pp. 1137–1143, Mar. 1992.

[4] D. Alukda, T. Sturgis, and B.-B. C. Youan, "Formulation of tenofovir-loaded functionalized solid lipid nanoparticles intended for HIV prevention," *J. Pharm. Sci.*, vol. 100, no. 8, pp. 3345–3356, Aug. 2011.

[5] J. N. Patton and A. F. Palmer, "Photopolymerization of Bovine Hemoglobin Entrapped Nanoscale Hydrogel Particles within Liposomal Reactors for Use as an Artificial Blood Substitute," *Biomacromolecules*, vol. 6, no. 1, pp. 414–424, Jan. 2005.

[6] A. Albanese, P. S. Tang, and W. C. W. Chan, "The Effect of Nanoparticle Size, Shape, and Surface Chemistry on Biological Systems," *Annu. Rev. Biomed. Eng.*, vol. 14, no. 1, pp. 1–16, 2012.

[7] W. H. De Jong and P. J. Borm, "Drug delivery and nanoparticles: Applications and hazards," *Int. J. Nanomedicine*, vol. 3, no. 2, pp. 133–149, Jun. 2008.

[8] K. S. Soppimath, T. M. Aminabhavi, A. R. Kulkarni, and W. E. Rudzinski, "Biodegradable polymeric nanoparticles as drug delivery devices," *J. Controlled Release*, vol. 70, no. 1–2, pp. 1–20, Jan. 2001.

[9] J. Meng, T. F. Sturgis, and B.-B. C. Youan, "Engineering tenofovir loaded chitosan nanoparticles to maximize microbicide mucoadhesion," *Eur. J. Pharm. Sci.*, vol. 44, no. 1–2, pp. 57–67, Sep. 2011.

[10] K. Cho, X. Wang, S. Nie, Z. (Georgia) Chen, and D. M. Shin, "Therapeutic Nanoparticles for Drug Delivery in Cancer," *Clin. Cancer Res.*, vol. 14, no. 5, pp. 1310–1316, Mar. 2008.

[11] R. H. Müller, K. Mäder, and S. Gohla, "Solid lipid nanoparticles (SLN) for controlled drug delivery – a review of the state of the art," *Eur. J. Pharm. Biopharm.*, vol. 50, no. 1, pp. 161–177, Jul. 2000.

[12] H. K. Makadia and S. J. Siegel, "Poly Lactic-co-Glycolic Acid (PLGA) as Biodegradable Controlled Drug Delivery Carrier," *Polymers (Basel)*, vol. 3, no. 3, pp. 1377–1397, Sep. 2011.

[13] L. Mu and S. . Feng, "A novel controlled release formulation for the anticancer drug paclitaxel (Taxol®): PLGA nanoparticles containing vitamin E TPGS," *J. Controlled Release*, vol. 86, no. 1, pp. 33–48, Jan. 2003.

[14] T. Chaowanachan, E. Krogstad, C. Ball, and K. A. Woodrow, "Drug Synergy of Tenofovir and Nanoparticle-Based Antiretrovirals for HIV Prophylaxis," *PLoS ONE*, vol. 8, no. 4, p. e61416, Apr. 2013.

[15] J.-M. Lu, X. Wang, C. Marin-Muller, H. Wang, P. H. Lin, Q. Yao, and C. Chen, "Current advances in research and clinical applications of PLGA-based nanotechnology," *Expert Rev. Mol. Diagn.*, vol. 9, no. 4, pp. 325–341, May 2009.

[16] K.-G. H. Desai and S. P. Schwendeman, “Active self-healing encapsulation of vaccine antigens in PLGA microspheres,” *J. Controlled Release*, vol. 165, no. 1, pp. 62–74, Jan. 2013.
[17] C. Wischke and S. P. Schwendeman, “Principles of encapsulating hydrophobic drugs in PLA/PLGA microparticles,” *Int. J. Pharm.*, vol. 364, no. 2, pp. 298–327, Dec. 2008.
[18] G. Niu, B. Cogburn, and J. Hughes, “Preparation and characterization of doxorubicin liposomes,” *Methods Mol. Biol. Clifton NJ*, vol. 624, pp. 211–219, 2010.
[19] S. Koudelka and J. Turánek, “Liposomal paclitaxel formulations,” *J. Control. Release Off. J. Control. Release Soc.*, vol. 163, no. 3, pp. 322–334, Nov. 2012.
[20] J. P. Schillemans, F. M. Flesch, W. E. Hennink, and C. F. van Nostrum, “Synthesis of Bilayer-Coated Nanogels by Selective Cross-Linking of Monomers inside Liposomes,” *Macromolecules*, vol. 39, no. 17, pp. 5885–5890, Aug. 2006.
[21] Y. Wang, S. Tu, A. N. Pinchuk, and M. P. Xiong, “Active drug encapsulation and release kinetics from hydrogel-in-liposome nanoparticles,” *J. Colloid Interface Sci.*, vol. 406, pp. 247–255, Sep. 2013.
[22] J. Park, S. H. Wrzesinski, E. Stern, M. Look, J. Criscione, R. Ragheb, S. M. Jay, S. L. Demento, A. Agawu, P. Licona Limon, A. F. Ferrandino, D. Gonzalez, A. Habermann, R. A. Flavell, and T. M. Fahmy, “Combination delivery of TGF-β inhibitor and IL-2 by nanoscale liposomal polymeric gels enhances tumour immunotherapy,” *Nat. Mater.*, vol. 11, no. 10, pp. 895–905, Jul. 2012.
[23] B. E. B. Jensen, L. Hosta-Rigau, P. R. Spycher, E. Reimhult, B. Städler, and A. N. Zelikin, “Lipogels: surface-adherent composite hydrogels assembled from poly(vinyl alcohol) and liposomes,” *Nanoscale*, vol. 5, no. 15, pp. 6758–6766, Jul. 2013.
[24] P. F. Kiser, G. Wilson, and D. Needham, “A synthetic mimic of the secretory granule for drug delivery,” *Nature*, vol. 394, no. 6692, pp. 459–462, Jul. 1998.
[25] W.-H. Tan and S. Takeuchi, “Monodisperse Alginate Hydrogel Microbeads for Cell Encapsulation,” *Adv. Mater.*, vol. 19, no. 18, pp. 2696–2701, 2007.
[26] S. Kazakov, M. Kaholek, I. Teraoka, and K. Levon, “UV-induced gelation on nanometer scale using liposome reactor,” *Macromolecules*, vol. 35, no. 5, pp. 1911–1920, 2002.

Author contributions

Renuka Ramanathan was a collaborator on this project and helped design and implement synthetic protocol modifications. Cryo-TEM images were created by Tamir Gonen and Matt Iadanza. The Methods paragraph on TEM analysis of NLGs was provided by Matt Iadanza. Figure 6 is courtesy of Renuka Ramanathan and used with permission.

Tables

Table 1: Expected parameters and specifications for NLGs synthesized via the final protocol along with the method of evaluation for each parameter.

Parameter	Specification	Method of evaluation
Size	~ 200 nm	DLS (one peak)
Polydispersity index (PDI)	~ 0.2	DLS (one peak)
Morphology	Hydrogel-core, lipid-shell structure	Detergent solubilization + DLS (two peaks) Cryo-TEM

Table 2: Review of synthetic steps modified during protocol development along with the specifications affected by the modifications, eventual outcome of each modification, and reference source.

Synthetic step	Specification	Strategy	Outcome	Reference
MLVs to ULVs	Size ~ 200 nm; PDI ~ 0.2	Bath sonication	Size > 200 nm; PDI > 0.2	Kazakov et al.
		Needle extrusion	Size ~ 200 nm; PDI ~ 0.2	Patton et al.
Removal of unencapsulated hydrogel constituents	Size ~ 200 nm; PDI ~ 0.2; no hydrogel slab	Dilution 20-25x	No NLG formation	Kazakov, Patton
		Ultracentrifugation	No NLG formation	Phillips et al.
		Addition of ascorbic acid, filtration, centrifugation	NLGs formed; size ~ 200 nm; PDI ~ 0.2	Schillemans et al.

Figures

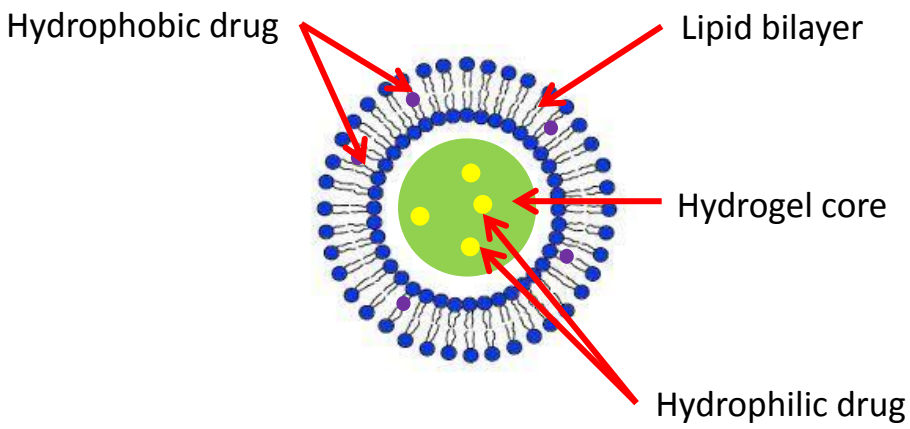

Figure 1: Schematic of NLG. A polymerized hydrogel core is surrounded by a single lipid bilayer. Hydrophilic drugs may be incorporated into the hydrogel core pre-polymerization, while hydrophobic drugs may be incorporated into the lipid bilayer during formation of the dry lipid film in NLG synthesis. In addition to the potential for combination delivery of hydrophobic and hydrophilic drugs, the NLG is expected to exhibit controlled release of hydrophilic drugs from the hydrogel core.

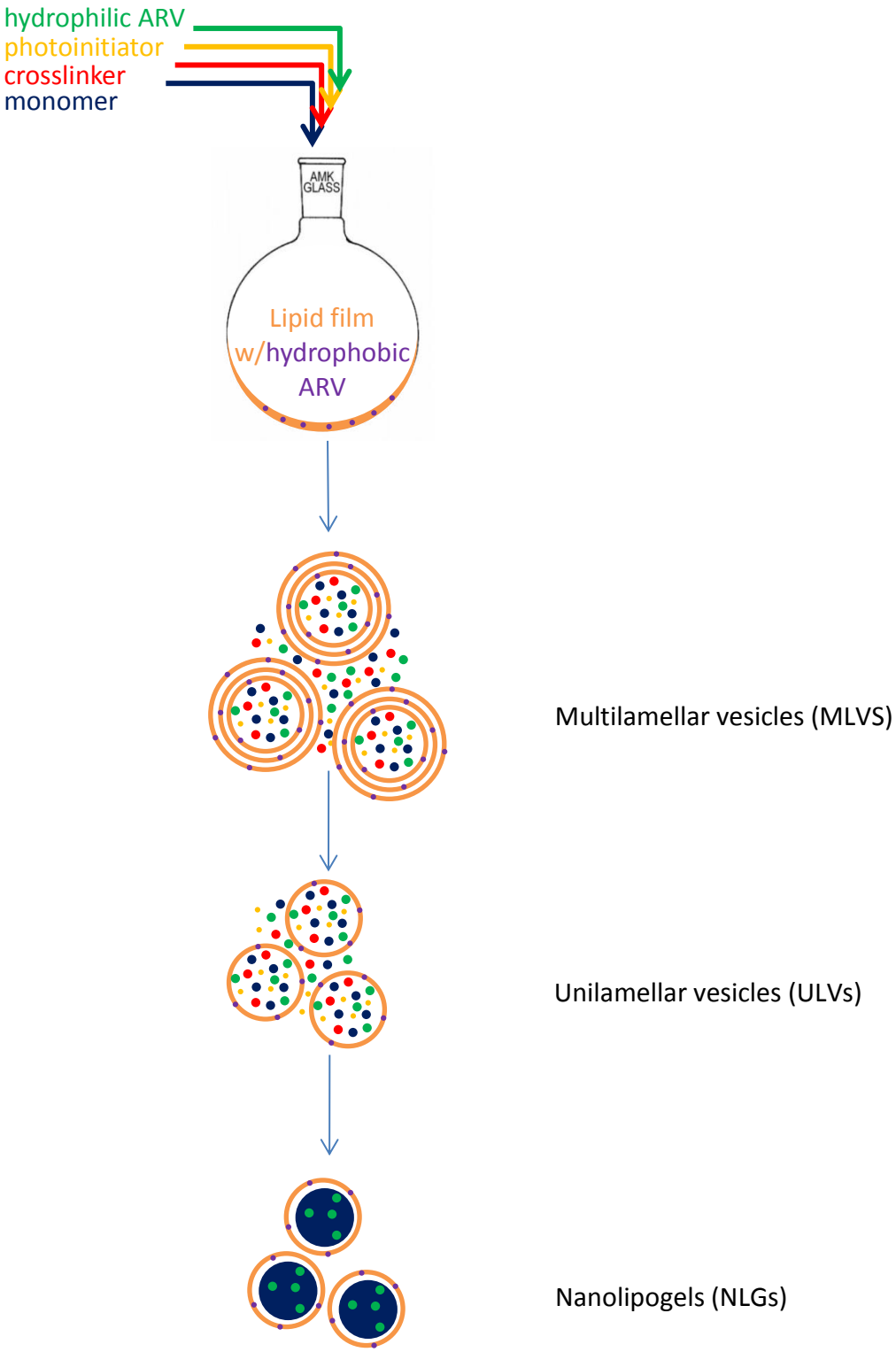

Figure 2: Schematic of nanolipogel synthesis by UV gelation within liposome reactors. A dry lipid film with hydrophobic drug is rehydrated with monomer, crosslinker, photoinitiator, and hydrophilic drug in buffer. This forms MLVs encapsulating hydrogel constituents. MLVs are reduced via one of many methods (bath sonication, extrusion, etc.) to ULVs encapsulating hydrogel constituents. After removal/inactivation of unencapsulated hydrogel constituents, ULVs are irradiated with UV light to polymerize the hydrogel core and form NLGs.

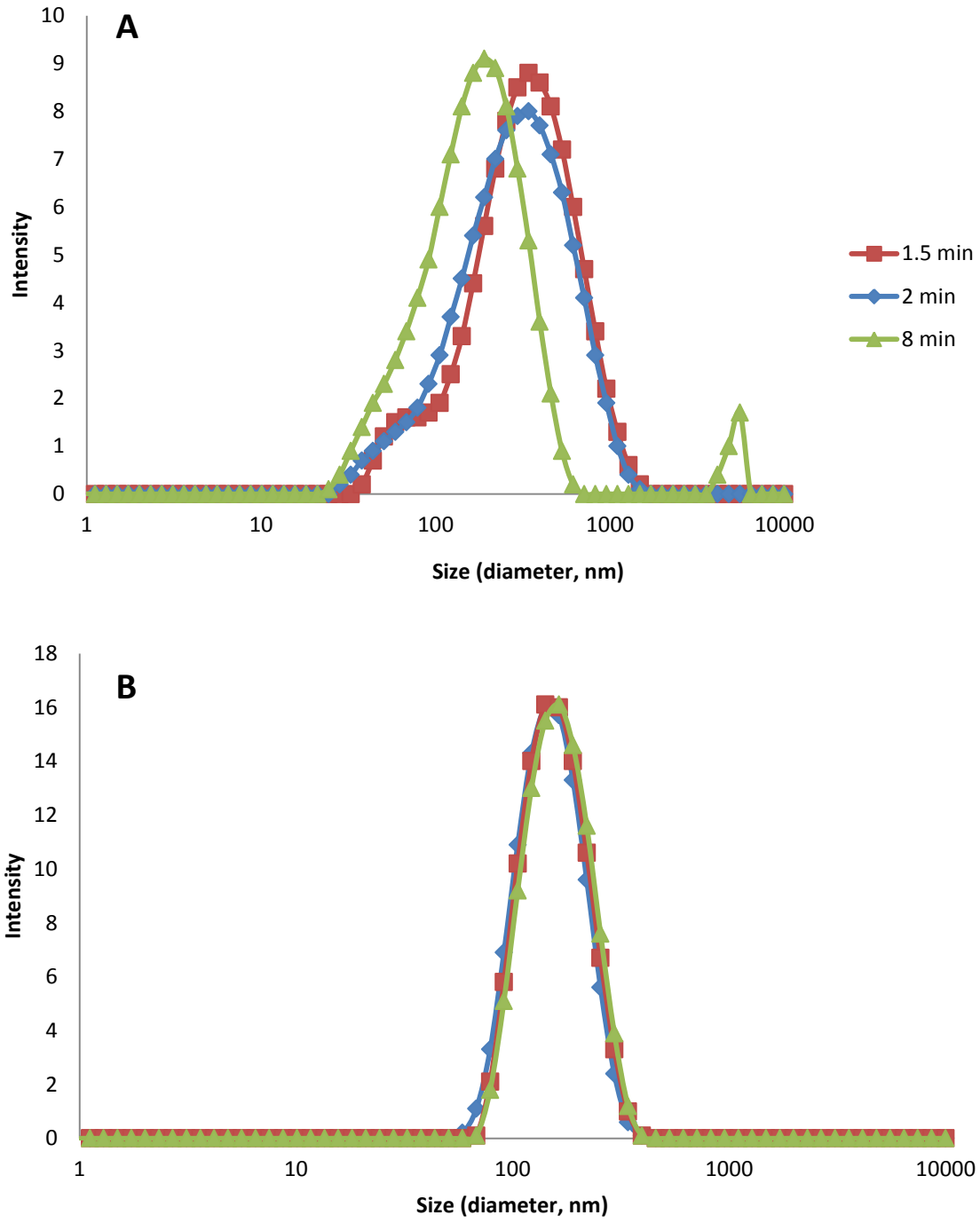

Figure 3: (A) Three populations of ULVs bath sonicated for 1.5 min, 2 min, and 8 min. Some time-dependent size control is apparent, but bath sonication results in high polydispersity (> 0.3) resulting from multiple extraneous peaks in the particle populations. PDI = 0.37 ± 0.05. (B) Three populations of ULVs needle extruded 11 times through a polycarbonate membrane with 200 nm pores. Unlike bath sonication, extrusion provides excellent size control as well as producing ULV populations with low PDI (< 0.2). The extraneous peaks and high PDI present in bath-sonicated ULV populations are eliminated. Size = 146.6 ± 5.8; PDI = 0.10 ± 0.01.

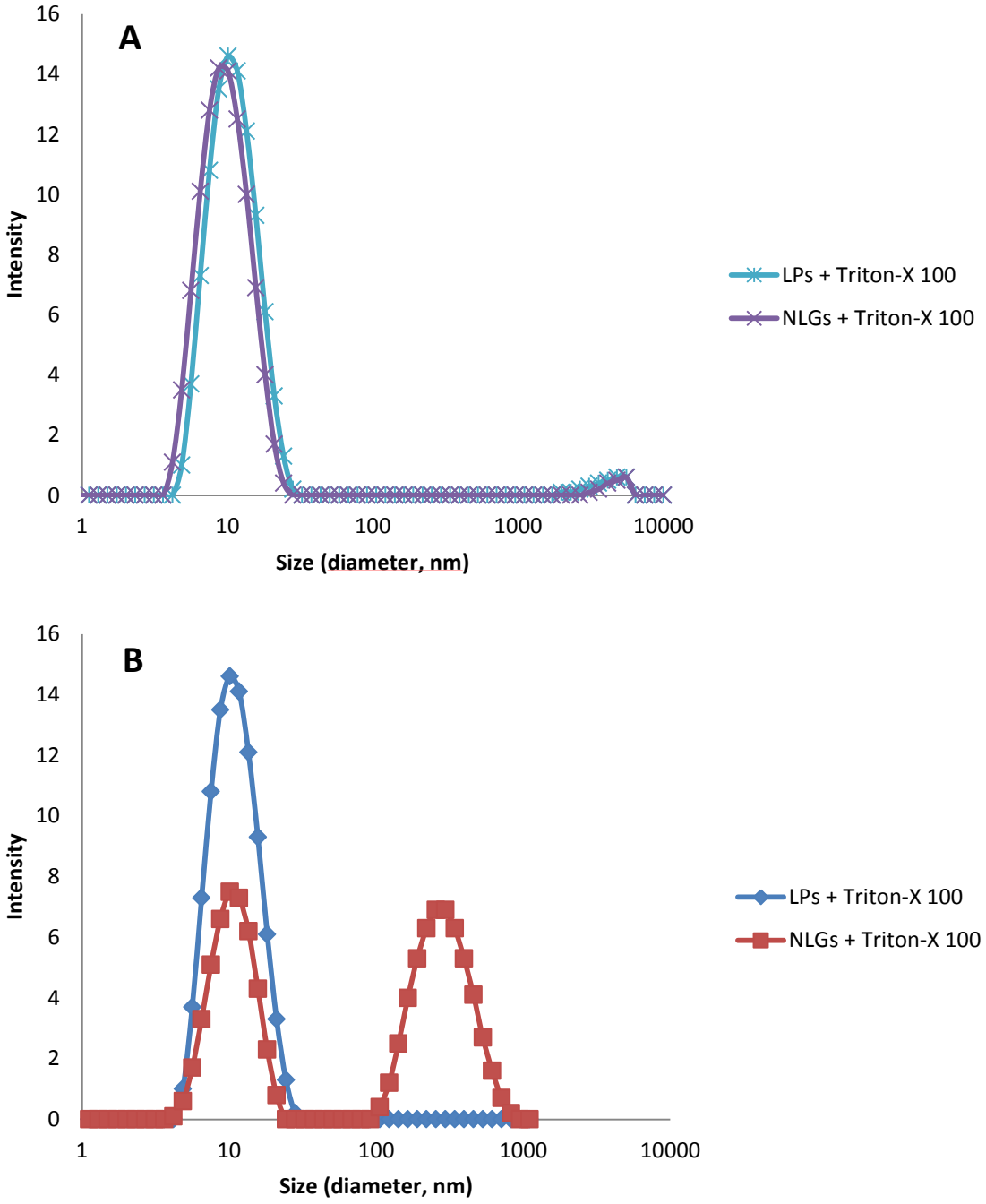

Figure 4: (A) Representative data of LPs and NLGs synthesized using ultracentrifugation and solubilized in 10-100 mM Triton-X 100. The LPs are fully reduced to mixed micelles. The NLGs are also fully reduced to mixed micelles with no bare hydrogel nanoparticle population visible, indicating failure of hydrogel core formation. (B) Representative data of LPs and NLGs formed using ascorbic acid addition, filtration, and centrifugation instead of ultracentrifugation solubilized in 10-100 mM Triton-X 100. While LPs are still entirely reduced to mixed micelles, NLGs are reduced to both mixed micelles and bare hydrogel nanoparticles, confirming the existence of a polymerized hydrogel core and validating the synthetic protocol.

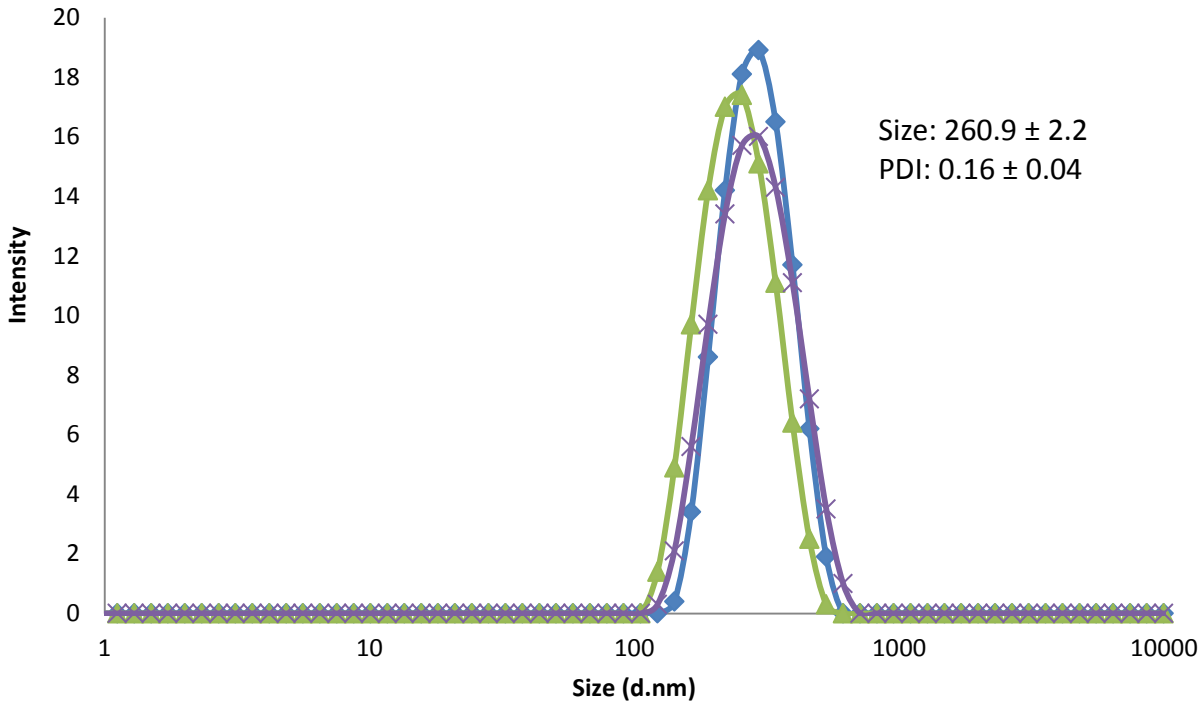

Figure 5: Three NLG populations synthesized using final protocol. NLG size is consistent and well controlled and PDI is within acceptable parameters. Size and PDI were brought under control by reduction of MLVs to ULVs using needle extrusion. Proper NLG formation and morphology was achieved by inactivating unencapsulated hydrogel constituents with ascorbic acids and then removing them with filtration and centrifugation. Size = 260.9 ± 2.2; PDI = 0.16 ± 0.04.

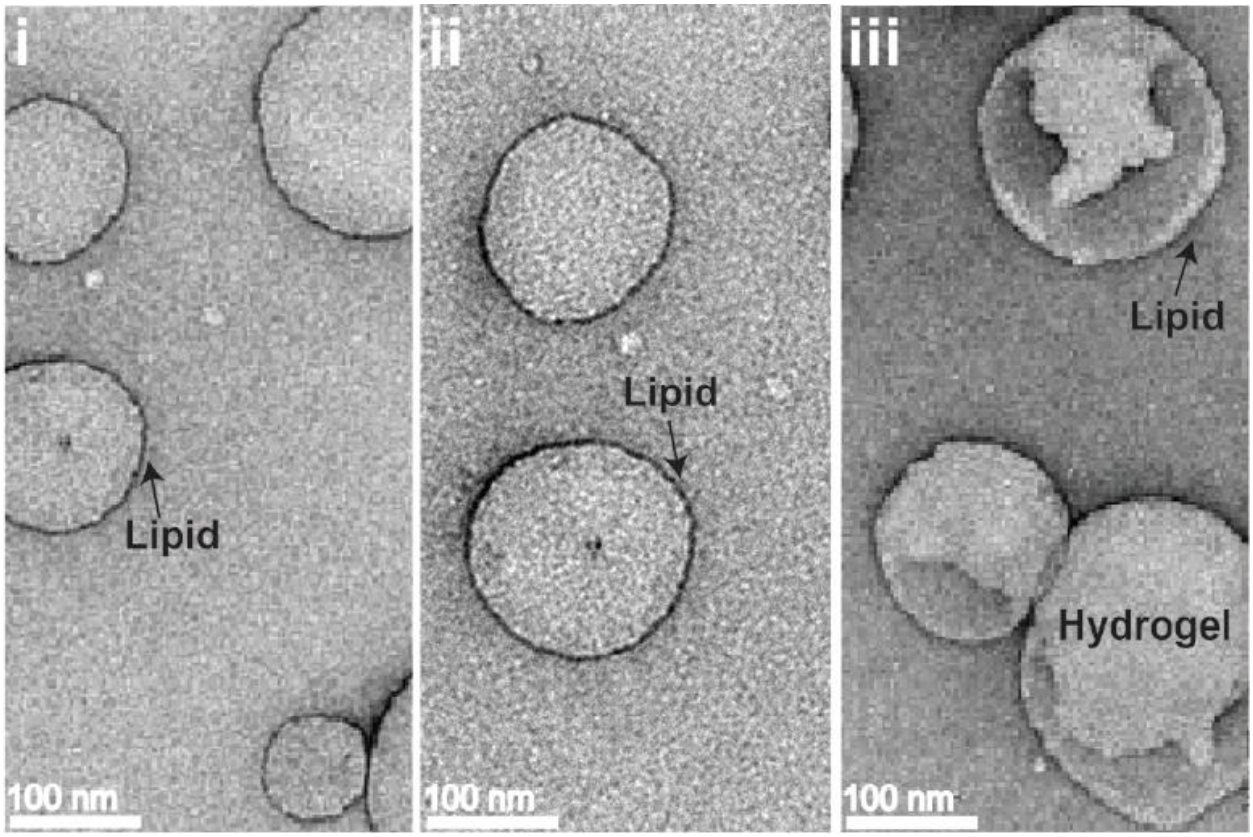

Figure 6: TEM images of liposomes (left), unilamellar vesicles (middle), and nanolipogels (right). Both the liposomes and the unilamellar vesicles appear smooth and flattened, while the nanolipogels appear flattened around a denser core, validating the presence of a polymerized hydrogel core within the lipid vesicle after UV irradiation.

CHAPTER 2: EVALUATION OF HYDROGEL SWELLING AS A MECHANISM FOR MODULATING DRUG RELEASE

Introduction

Hydrogels are porous crosslinked networks of hydrophilic polymers able to absorb and release large amounts of water relative to their polymer weight (>20%) while maintaining their morphological structure [27]. As polymers, hydrogels are composed of one or more types of monomer and crosslinker. The porosity of hydrogels is dependent upon a number of factors, including number of physical crosslinks within the hydrogel and hydrophilicity of the constituents [28]. Flux of water into and out of the hydrogel leads to swelling and deswelling of the crosslinked mesh with corresponding changes in the crosslinked characteristic length [29]. Swelling and deswelling behavior can be modulated by varying crosslinking type and density, or be made responsive to a wide variety of stimuli such as changes in pH or temperature, antibody binding, or ultrasound [27]. Furthermore, hydrogels can be made to degrade in response to similar environmental stimuli. This behavior and versatility makes hydrogels ideal biomaterials for drug encapsulation and release. Bulk and particulate hydrogel systems have successfully encapsulated and released viable whole cells for tissue engineering applications [25], large proteins including functional hemoglobin as a red blood cell substitute [5], combinations of small-molecule drugs (protein inhibitor) and small proteins (cytokine) for cancer therapeutics [22], and small-molecule hydrophobic drugs (doxorubicin) [24].

Swelling in hydrogels can have significant effects on drug release. Glassy (i.e. dried) hydrogels with encapsulated drug exhibit non-Fickian diffusion of drug when placed in an aqueous environment. This they exhibit release behavior that cannot be modeled or completely explained by Fick's laws of diffusion, which concentration and flux to a diffusion coefficient D. Swelling of the hydrogel can cause burst release of drug during the initial stages of release, particularly if

the drug is hydrophilic and resides in the aqueous phase of the hydrogel rather than being closely associated with the polymer mesh. The diffusion rate of water inward, coupled to the diffusion of drug outward, is mediated by rate of characteristic crosslinker length increase [27], [30]. This mechanism of drug release differs significantly from release out of PLGA systems or liposomes, which exhibit release either as Fickian diffusion from intact particles or as a result of vehicle degradation (biodegradation or lysis within cells). On the other hand, fully swollen hydrogels can exhibit Fickian diffusion of drug in an aqueous environment, as no overall swelling of the hydrogel occurs, meaning that the diffusion rate of water inward is not mediated by rate of characteristic crosslinker length change [1], [27], [31]. A diffusion coefficient D can be used to describe the diffusive behavior of the drug and the characteristic crosslink length does not change over time. Initial burst release can still occur in instances of large pore size relative to drug radius, but this limitation can be partially addressed by varying the ratio of crosslinker to monomer in the hydrogel to produce a smaller pore size. A twofold increase in crosslinker concentration in polyacrylamide gel can produce up to a 10% difference in small-molecule drug release over time [32] An increase in crosslinker concentration can also cause a Fickian to non-Fickian shift [27], [32].

Bulk hydrogels and hydrogel microparticulate systems have been studied extensively in literature for delivery of biological agents and small-molecule drugs. Hydrogel swelling can act as a mechanism for drug release in these systems, as flux of water into the hydrogel is exchanged for drug diffusion out of the hydrogel. However, little investigation has been performed on drug release from nanoparticulate hydrogel systems as a result of hydrogel swelling, specifically on whether or not differences in hydrogel swelling lead to differences in rate and amount of drug release. While hydrogel swelling can be the primary driving factor behind drug release at the

macro- and micro-scale, at the nano-scale many factors other than hydrogel swelling may affect drug release. These factors include hydrogel porosity, concentration of loaded drug per mass, surface area to volume ratio of the nanoparticle, and monomer to crosslinker ratio in the nanoparticle. This study evaluated the extent of the influence crosslinker-dependent hydrogel swelling has on NLG release of azidothymidine (AZT), a small-molecule antiretroviral used in HIV treatment and prophylaxis. Steps in this evaluation include establishment of differential hydrogel swelling and equilibrium water content (EWC) based on crosslink density, mechanical analysis of bulk hydrogel shear response as a qualitative way to determine number of crosslinks, and loading and release of AZT into NLGs over time. (Table 1)

Materials and methods

Materials

Egg phosphatidylcholine (EPC); 1,2-dioleoyl-*sn*-glycero-3-phospho-(1'-rac-glycerol) (DOPG); and all needle extruder components were purchased in chloroform from Avanti Polar Lipids. Acrylamide (AAm) monomer, methylene-bis-acrylamide (MBA) crosslinker, and diethoxyacetophenone (DEAP) photonitiator were purchased in aqueous solution from Sigma-Aldrich. Azidothymidine (AZT), a nucleoside reverse transcriptase inhibitor used here as a model small-molecule hydrophilic drug, was purchased from Sigma-Aldrich. Water used in buffer solution was purified using a Milli-Q purification system (Millipore Corporation).

Bulk hydrogel synthesis and equilibrium water content (EWC) testing

Bulk hydrogels were synthesized by combining AAm and MBA in water at varying ratios (Table 1) below and 2.17 ul/ml of DEAP in buffer. The solution was plated into a Petri dish and exposed to ultraviolet light until polymerization was complete. The bulk hydrogels were sectioned, weighed, and placed in 15 ml deionized water. At each timepoint, hydrogel sections were removed from the water, patted dry, and re-weighed to determine changes in water content over time. Water content at each time point was determined by dividing the timepoint mass by the initial mass:

$$\mathrm{EWC} = \frac{\text{timepoint mass (mg)}}{\text{original mass (mg)}}$$

Rheology of bulk hydrogels

Bulk hydrogels were synthesized as described above in Petri dishes. After polymerization, each hydrogel was rinsed in distilled water and cut around its circumference approximately 2 mm from the edge of the Petri dish in order to minimize edge effects during rheological analysis. Each hydrogel in its Petri dish was then subjected to a frequency sweep of 1-100 rad/s on an AR-G2 rheometer (TA Instruments) using a 40 mm smooth parallel plate at a 2% fixed strain rate and a gap of 4 mm. Storage modulus (G') and loss modulus (G") were measured during the frequency sweep.

Drug encapsulation and release studies in nanolipogels

Nanolipogels were synthesized via UV gelation in liposome reactors. Briefly, EPC and DOPG in chloroform at a 9:1 mass/mass ratio film were combined with MVC at 10% lipid mass and placed on a rotary evaporator (Buchi) to form a dry drug-loaded lipid film. The lipid film was then rehydrated with AAm and MBA in varying ratios, AZT at 10% lipid mass, and DEAP in buffer to 5 mg lipid/ml buffer solution, forming multilamellar vesicles. The multilamellar vesicles were reduced to unilamellar vesicles encapsulating hydrogel components, AZT, and MVC via extrusion using a hand-held needle extruder. Ascorbic acid was added to the unilamellar vesicles to prevent external polymerization and the solution was then exposed to UV light, forming combination AZT/MVC nanolipogels. The nanolipogels were filtered and collected via centrifugation at 14,000g for 10 minutes, and the supernatant was saved for encapsulation efficiency analysis by HPLC.

Drug-loaded nanolipogels were placed in a membrane-capped dialysis tube with a 1 kDA molecular weight cutoff (GE USA). The tube was inverted cap-down into 5 ml buffer in a 50 ml conical tube, which was placed on a shaker table rotating at 120 rpm at 37°C. At each timepoint,

the buffer solution was vortexed and 100 ul was removed and replaced with fresh buffer. Timepoint buffer samples were analyzed using high pressure liquid chromatography (HPLC). Drug release data was analyze in two ways. The first involved normalizing total released drug to total lipid content of recovered NLGs. Release level at each timepoint was calculated by the following equation:

$$\text{Release}\left(\frac{\text{mg}}{\text{mg}}\right) = \frac{\text{total AZT released (mg)}}{\text{total lipid yield (mg)}}$$

where

$$\text{Total AZT released (mg)} = \text{HPLC conc.}\left(\frac{\text{mg}}{\text{ml}}\right) \times \text{release buffer volume (ml)}$$

and

$$\text{Total lipid yield (mg)} = \text{Bartell assay conc.}\left(\frac{\text{mg}}{\text{ml}}\right) \times \text{total sample volume (ml)}$$

The second approach involved expressing released drug as a percentage of total drug loaded into the NLGs as determined by HPLC. Release level at each timepoint was analyzed via the following equation:

$$\text{Release}(\%) = \frac{\text{Total AZT released (mg)}}{\text{Total AZT loaded (mg)}} \times 100$$

where

$$\text{Total AZT released (mg)} = \text{HPLC timepoint conc.}\left(\frac{\text{mg}}{\text{ml}}\right) \times \text{release buffer volume (ml)}$$

and

$$\text{Total AZT loaded (mg)}$$

$$= \text{original AZT loaded (mg)} - \left(\text{HPLC supernatant conc.} \left(\frac{\text{mg}}{\text{ml}}\right) \times \text{total supernatant volume (ml)}\right)$$

HPLC method development

AZT release from nanolipogels over time was quantified on an HPLC (Shimadzu America) with a C18 column using a 10 ul injection volume. Samples were solubilized in 72%: 28% v/v 0.045% trifluoroacetic acid (TFA) in HPLC grade water : 0.036% TFA in HPLC grade acetonitrile. Flow rate was 1 ml/min and the retention time of AZT was approximately 4.2 minutes. Drug release at each timepoint was determined quantitatively using standards developed on HPLC by spiking free drug into blank nanolipogel supernatant. Total drug loaded into the nanolipogels was determined quantitatively by HPLC of supernatant from drug-loaded nanolipogels.

Lipid content determination of nanolipogels

Mass recovery of nanolipogels was determined using a Bartell assay to quantify phosphorous content. Briefly, nanolipogel samples were digested in 8.9 N H_2SO_4 at 200°C, re-solubilized in H_2O_2, cooled, and complexed with ammonium molybdate tetrahydrate and ascorbic acid. Lipid content was quantified on a UV-Vis spectrophotometer (Thermo Scientific) at 820 nm using a prefabricated phosphorus standard.

Results and Discussion

Lower crosslinker concentration leads to higher EWC and greater degree of swelling

Bulk hydrogels were synthesized with varying ratios of MBA to a fixed concentration of AAm in order to produce hydrogels with differing equilibrium water content and swelling rates. When polymerized, bulk hydrogels with higher concentrations of MBA (≥ 35 mM MBA) were visually more opaque and more rigid to the touch than hydrogels with lower MBA concentrations (data not shown). Hydrogels with MBA at 70 mM or more were brittle and often broke apart during tests of EWC and rheology. In contrast, hydrogels with low MBA concentrations were clearer visually and more pliable to the touch. At low MBA concentrations (3.5 mM-8.75 mM), the hydrogels flowed when the Petri dishes holding them were tilted, though they still held together as a solid. Qualitatively, hydrogels at 1.4 mM MBA and below appeared to behave entirely like viscous liquids. These observations provided visual and qualitative conformation that lower MBA concentrations in the initial hydrogel solution produced less solid hydrogels.

Rheological studies of bulk hydrogels

Rheological data confirms quantitatively the observation that hydrogels with low MBA concentrations behave more like liquids than like solids under low levels of shear. The frequency sweep was conducted from 1-100 rad/s in order to document the behavior of variably crosslinked hydrogels across a wide shear range. At low shear (1 rad/s) hydrogels with low MBA concentrations had significantly lower storage moduli (G') and loss moduli (G") than hydrogels with high MBA concentrations (Figure 2, Table 3). Notably, a tenfold difference in MBA concentration (3.5 mM vs. 35 mM) resulted in approximately a tenfold difference in G' (Table 2). The representative frequency-sweep data for 1.4 mM MBA hydrogels shows an intersection point where G' rises above G" with increasing frequency (Figure 3). This behavior is indicative

of a liquid, as the loss modulus G" is the dominant determinant of mechanical behavior in liquids while G' is dominant in solids [33]. This is apparent when the G'/G" ratio shows a trend towards increasing with increasing MBA concentration. By contrast, 14 mM and 140 mM MBA hydrogels show no such intersection point, with G' tenfold higher than G", indicating solid-like behavior. This data confirms the qualitative observation that hydrogels with low MBA concentrations exhibit greater flow characteristics and are physically less rigid than hydrogels with high MBA concentrations. Higher values of G' relative to G" provide a quantitative representation of higher numbers of crosslinks within the bulk hydrogel. Varying crosslinker concentrations result in clear differences in mechanical properties and swelling capacity that may lend themselves to differences in release of encapsulated small-molecule drugs.

Diffusion coefficients of AZT from hydrogels of varying crosslinker concentration show limited differences

EWC data shows hydrogels with low MBA concentrations swell to a greater extent and take on more water relative to their original mass than hydrogels with high MBA concentrations (Figure 1). The gels are fully swollen around 24 hours. This data indicates that lower MBA concentration results in a greater flux of water into the bulk gel. Given that a greater flux of water into the hydrogel should correspond to a greater release of drug out of the hydrogel, we would expect to see higher levels of drug release from less heavily crosslinked NLGs if hydrogel swelling is the primary factor driving AZT release.

We estimated the diffusion coefficient of AZT in hydrogels from the EWC testing given a certain set of assumptions. The first of these assumptions is that drug diffusion would be Fickian, as neither the slab hydrogels nor the NLGs would be glassy (dried) during EWC and drug release tests. Assuming Fickian diffusion allows us to correlate AZT diffusion coefficient based on

EWC, which varies based on swelling over time. The second assumption is the calculation of diffusion coefficients in slab hydrogels rather than in spherical particulate hydrogel systems. Massing and re-massing of hydrogel slabs was the most facile way to conduct EWC tests. Therefore, the calculated diffusion coefficients may not be numerically similar to the actual diffusion coefficients of AZT out of NLGs. However, they should provide a qualitative comparison and trend of AZT diffusion coefficients in low and high crosslinker hydrogel systems. Weber [34] developed the following equation for one-dimensional Fickian diffusion of solute within a slab of polyacrylamide hydrogel:

$$\frac{D_g}{D_w} = \left(1 - \frac{r_s}{\xi}\right) exp\left(-Y\left(\frac{v_2}{1 - v_2}\right)\right)$$

where

D_g = diffusion coefficient of solute in hydrogel

D_w = diffusion coefficient of solute in water

r_s = radius of solute

ξ = crosslinked network characteristic length

Y = ratio of volume of water required for transitional movement to average free volume per liquid molecule

$v_2 = 1/\text{EWC}$

The following assumptions and substitutions are made into the equation:

D_w for AZT = 4.84×10^{-4} cm^2/min

r_s for AZT = 3.84 Å

ξ constant [27]

Y ~1 [34]

These assumptions and substitutions result in the following simplified equation for the diffusion coefficient of AZT in hydrogel given the EWC:

$$D_g = \exp\left(-\frac{v_2}{1-v_2}\right) * (4.84 \times 10^{-4})$$

Calculating D_g for AZT in low and high crosslink hydrogels reveals slightly lower values of D_g for higher crosslink hydrogels (Table 2), indicating that AZT may not diffuse as readily out of NLGs with a higher MBA concentration than NLGs with a lower MBA concentration. However, the calculated values of D_g are not that different from each other nor from D_w (all have the same order of magnitude), so it is also possible that no statistically significant differences in AZT diffusion based on hydrogel swelling will emerge.

AZT release from NLGs is not dependent upon MBA concentration; however, higher MBA concentration correlates to higher encapsulation efficiency

With the lower-crosslinked bulk hydrogels swelling to a greater extent and behaving more like a liquid mechanically, we hypothesized that lower-crosslinked hydrogels would release encapsulated drug at a faster rate or to a greater extent over time than more highly crosslinked hydrogels. However, we did not observe a correlation between variable crosslinking in NLGs and release. Drug release normalized to percent of drug loaded does not show significant differences between higher MBA and lower MBA NLGs (Figures 4 and 5), which would seem to invalidate swelling as a significant mechanism of NLG drug release If swelling rate were a primary force governing drug release, we would expect to see NLGs with lower MBA concentrations releasing drug faster and to a greater extent than NLGs with higher MBA concentrations. Since rate and extent of drug release evaluated by percent release are similar for

variably crosslinked NLGs, we cannot conclude that hydrogel swelling plays a primary role in AZT release from NLGs.

Drug release normalized to lipid mass shows a trend towards NLGs with higher MBA concentrations loading and releasing greater amounts of AZT than NLGs with lower MBA concentrations (Figures 6 and 7). High MBA NLGs exhibited significantly lower particle yield (lipid mass) than MBA NLGs, but exhibited similar levels of drug loading as low MBA concentrations. This indicates that high crosslinker NLGs may be more efficient and effective at drug entrapment.

Conclusions

Hydrogel swelling does not appear to be the main driving force behind drug release from NLGs. NLGs with high and low MBA concentrations show similar levels of drug loading and release. Furthermore, the drug release profiles are highly similar in shape, indicating no differences in rate of release based on MBA concentration. The drug release observations correlate with the similar values of D_g found for AZT through the variably crosslinked slab hydrogels, both indicating a lack of swelling influence on release. However, NLGs with high MBA concentration appear to exhibit higher encapsulation efficiency than low MBA NLGs. Given this observation, the most likely candidate for the driving factor in NLG drug release is drug concentration in individual NLGs, which is significantly higher in high crosslinker NLGs given their higher encapsulation efficiency. Lower lipid yield would also lead to a lower concentration of high MBA NLGs in release studies, since NLGs were portioned into the dialysis kits by volume. These factors may have caused greater sink conditions for the NLGs and contributed to higher levels of drug release over time. Another potential factor is variable porosities of the hydrogel cores in their semi-swollen state after NLG synthesis. If the pores are significantly larger than the drug hydrodynamic radius in both NLG populations, porosity would have a greater effect on initial drug release than hydrogel swelling. It is also possible that hydrogel swelling in slab-shaped samples on the macroscale (as examined in the EWC testing) is not the same as or directly comparable to hydrogel swelling in spherical particles on the nanoscale, due to differences in scale, shape, and size of the hydrogels in question. Fick's law for diffusion differs in spherical coordinates as compared to the one-dimensional equation used to determine diffusion coefficients in AZT for variably crosslinked bulk hydrogels. The assumptions and

parameters of this equation are highly limited by the fact that they deal with a slab hydrogel, making the comparison to a spherical hydrogel system rather tenuous.

The higher encapsulation efficiency of drug seen in high crosslinker NLGs can similarly be due to a host of factors. Given the greater swelling exhibited in low crosslinker NLGs, it is important to consider the possibility of rapid diffusion of AZT out of low crosslinker NLG cores during the polymerization process itself. As higher numbers of crosslinks form in high crosslinker NLGs, greater levels of entrapment may impede diffusion of AZT out of the NLGs during polymerization to an extent which does not occur in low crosslinker NLGs. This study also did not take into account the specific location of drug within the NLG. It was presumed that the majority of encapsulated drug would reside within the hydrogel core, but given that the hydrogel core is often smaller in diameter than the surrounding lipid shell, it is impossible to rule out the possibility that some drug may in fact reside in the aqueous space between the core and the shell. Given the greater sink conditions for high crosslinker NLGs, it is possible that the increased release over time is a result of AZT being driven solely through the lipid shell.

Limitations of this study include the fact that the bulk hydrogels and NLGs were neither fully glassy nor fully swollen during testing, making it difficult to establish Fickian vs. non-Fickian diffusion. Swelling behavior may in fact have a greater influence on drug release from dried (glassy) NLGs than was apparent from these studies. A further limitation is the attempted translation of slab bulk hydrogel properties to spherical nanoscale hydrogels. While it is reasonable to have confidence that crosslinker density would remain relatively similar between the two systems, other factor such as size, shape, and varying mechanisms of diffusion have not been taken into account. Also not taken into account in terms of diffusion is the presence of the lipid shell, which is difficult to model on the macroscale. Nonetheless, the study has produced a

reproducible population of hydrogel-core, lipid-shell NLGs that successfully encapsulate and release small-molecule hydrophobic drugs, with an increase in crosslinker concentration in the hydrogel core corresponding to higher efficiency in drug encapsulation and higher levels of drug release.

References

[27] P. Gupta, K. Vermani, and S. Garg, "Hydrogels: from controlled release to pH-responsive drug delivery," *Drug Discov. Today*, vol. 7, no. 10, pp. 569–579, May 2002.

[28] W. E. Hennink and C. F. van Nostrum, "Novel crosslinking methods to design hydrogels," *Adv. Drug Deliv. Rev.*, vol. 64, Supplement, pp. 223–236, Dec. 2012.

[29] K. Kabiri, H. Omidian, S. A. Hashemi, and M. J. Zohuriaan-Mehr, "Synthesis of fast-swelling superabsorbent hydrogels: effect of crosslinker type and concentration on porosity and absorption rate," *Eur. Polym. J.*, vol. 39, no. 7, pp. 1341–1348, Jul. 2003.

[30] L. Serra, J. Doménech, and N. A. Peppas, "Engineering design and molecular dynamics of mucoadhesive drug delivery systems as targeting agents," *Eur. J. Pharm. Biopharm.*, vol. 71, no. 3, pp. 519–528, Mar. 2009.

[31] B. Amsden, "Solute Diffusion within Hydrogels. Mechanisms and Models," *Macromolecules*, vol. 31, no. 23, pp. 8382–8395, Nov. 1998.

[32] K. S. Soppirnath and T. M. Aminabhavi, "Water transport and drug release study from cross-linked polyacrylamide grafted guar gum hydrogel microspheres for the controlled release application," *Eur. J. Pharm. Biopharm.*, vol. 53, no. 1, pp. 87–98, 2002.

[33] C. A. Grattoni, H. H. Al-Sharji, C. Yang, A. H. Muggeridge, and R. W. Zimmerman, "Rheology and Permeability of Crosslinked Polyacrylamide Gel," *J. Colloid Interface Sci.*, vol. 240, no. 2, pp. 601–607, Aug. 2001.

[34] L. M. Weber, C. G. Lopez, and K. S. Anseth, "The effects of PEG hydrogel crosslinking density on protein diffusion and encapsulated islet survival and function," *J. Biomed. Mater. Res. A*, vol. 90, no. 3, pp. 720–729, Sep. 2009.

Tables

Table 1: Investigations into swelling properties of hydrogels and their effects on AZT release along with their methods of evaluation, parameters sought, and reference.

Investigation	Method of evaluation	Parameters	Reference
Differential bulk hydrogel swelling	Equilibrium water content (EWC) testing	Hydrogel mass (mg)	Soppirnath et al., Rao et al.
Mechanical differences in bulk hydrogel	Rheology	G', G" (Pa)	Gautreau et al., Grattoni et al.
Encapsulation and release of AZT in NLGs	HPLC	Mass AZT released (mg)	dos Santos et al.

Table 2: Diffusion coefficients of AZT in slab hydrogels as related to EWC.

[MBA]	D_g (cm^2/min)
35 mM	1.03E-04
8.75 mM	1.68E-04

Table 3: G', G" and G'/G" ratio for low crosslinker and high crosslinker hydrogels under 1 rad/s frequency shear.

	G'	G"	G'/G"
3.5 mM	157.2 ± 127.2	26.2 ± 21.1	6.3 ± 2.5
35 mM	1435.0 ± 133.5	144.2 ± 25.8	10.3 ± 2.6
p-val	0.000280292	0.00404286	0.128796

Figures

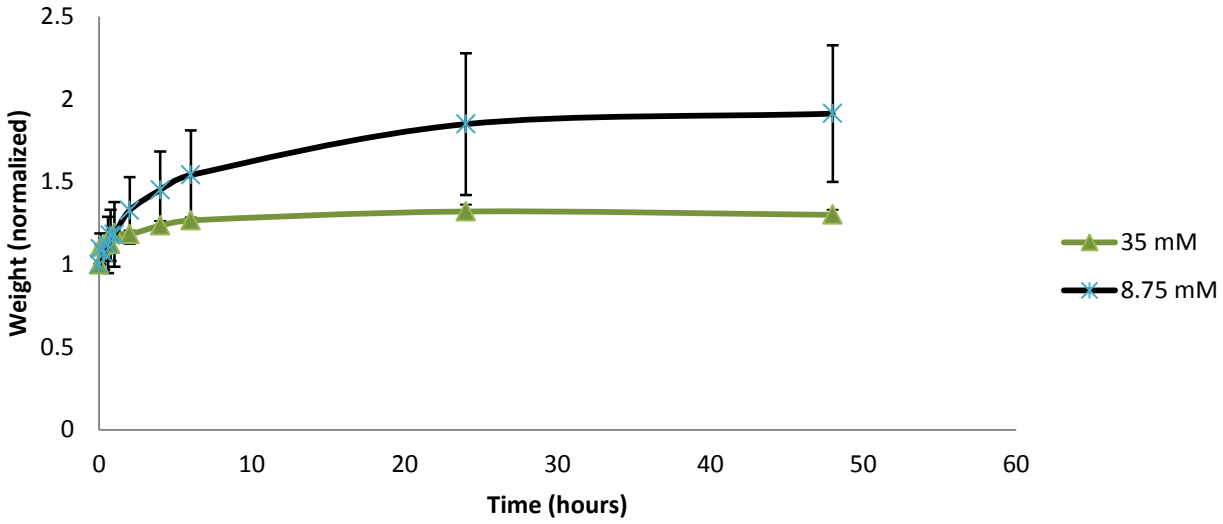

Figure 1: EWC testing of bulk hydrogels with varying MBA concentration. Lower MBA concentration leads to a greater degree of swelling and consequently a higher EWC after a 48-hour period. Higher MBA concentration leads to a lower degree of swelling and lower EWC in the same time frame.

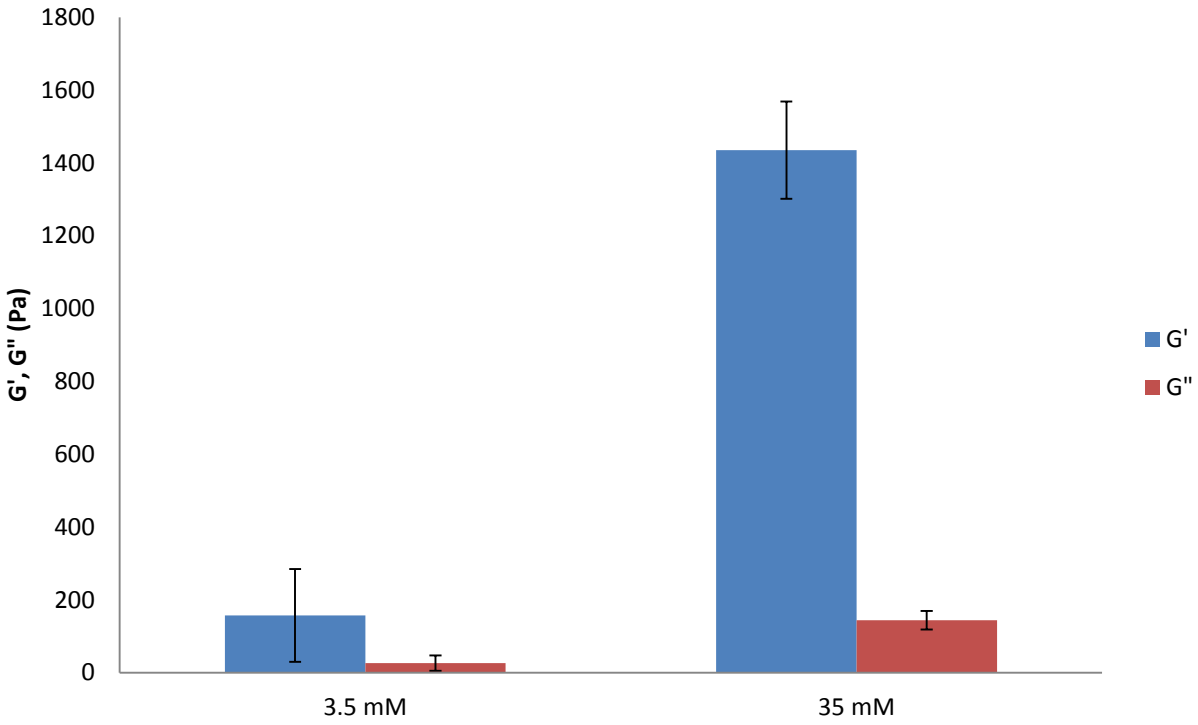

Figure 2: Rheology of bulk hydrogels of varying MBA concentration under low shear from angular frequency sweep (1 rad/s). Lower MBA concentration results in lower values of G' and G" and a smaller ratio between G' and G", indicative of more liquid-like behavior and lower crosslink density.

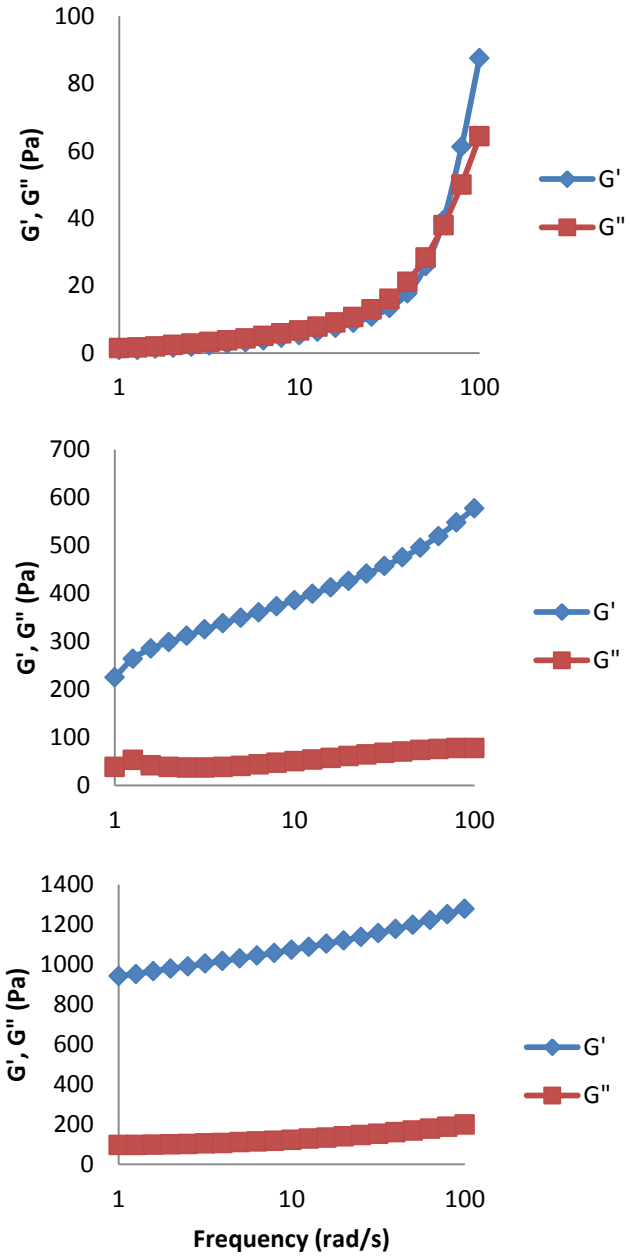

Figure 3: Representative rheology data for bulk hydrogels with (top) 1.4 mM, (middle) 14 mM, and (bottom) 140 mM MBA concentration, frequency sweep from 1-100 rad/s. Note the crossover between G' and G" in the 1.4 mM hydrogel. G" dominates hydrogel behavior at low frequencies while G' takes over at higher frequencies, indicative of a liquid. A tenfold difference between G' and G", as seen in the 14 mM and 140 mM hydrogels, is indicative of a solid.

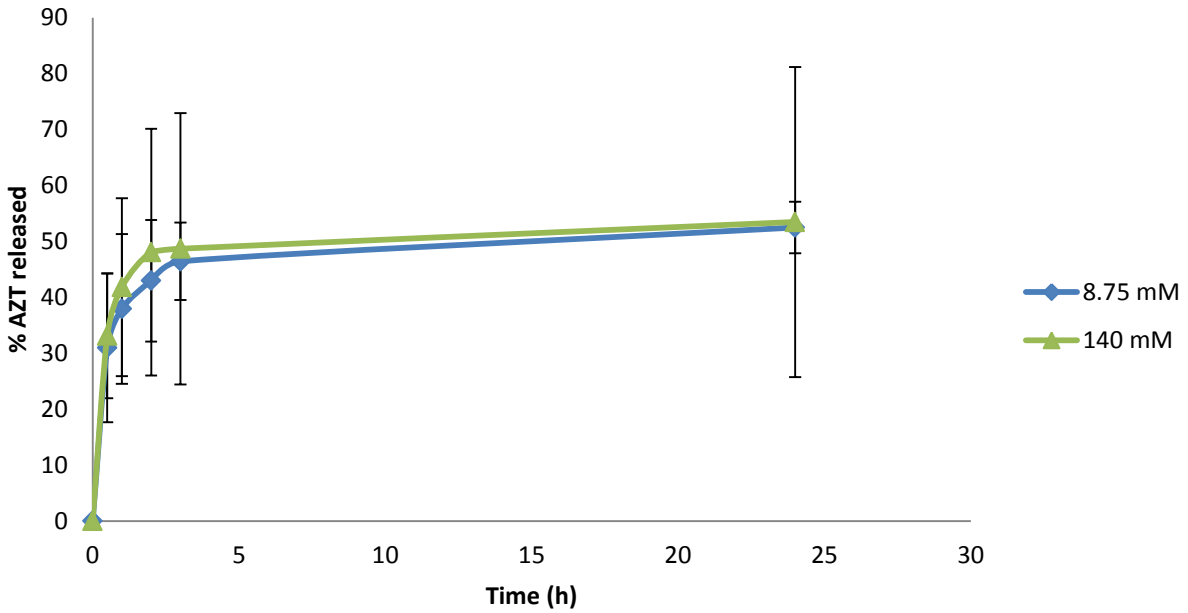

Figure 4: AZT release from variably crosslinked NLGs as a percent of total drug encapsulated. No trend emerges; the release is identical from both NLG populations regardless of crosslinker concentration.

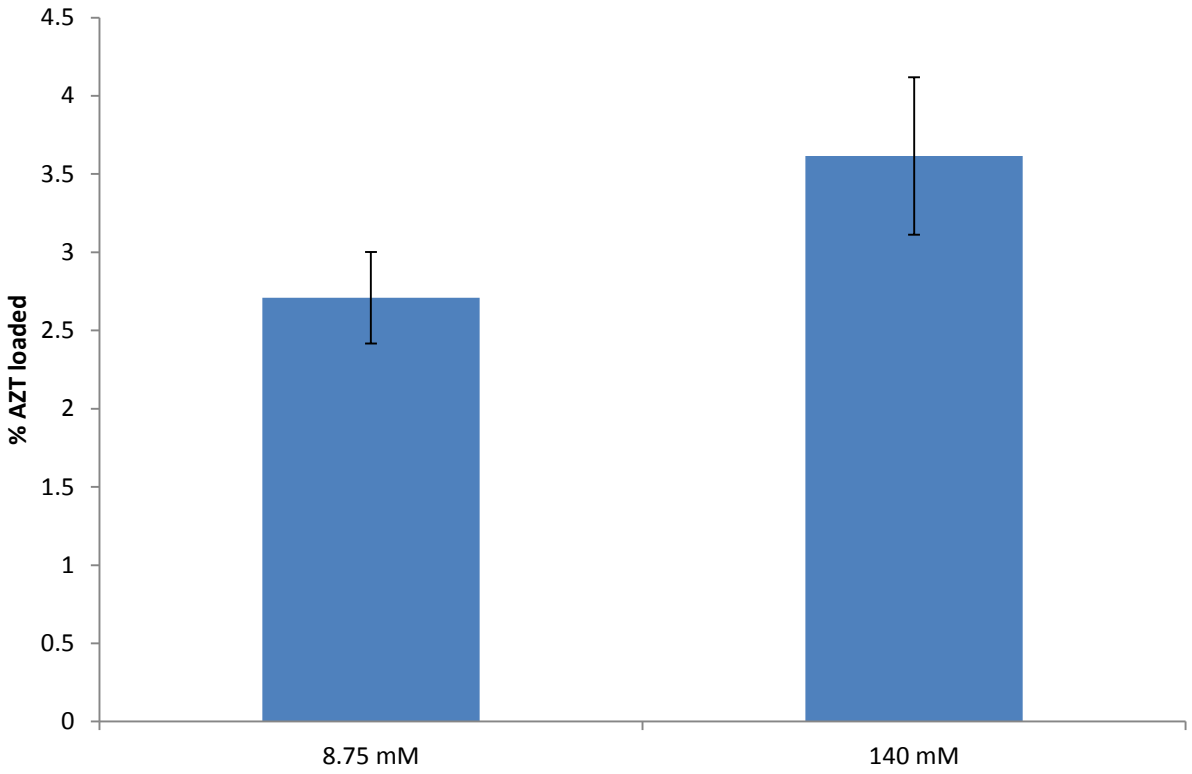

Figure 5: AZT drug loading in variably crosslinked NLGs normalized to percent of drug initially loaded during synthesis. Mass of drug loaded into 8.75 mM NLGs was 0.027 ± 0.003 mg, while mass of drug loaded into 140 mM NLGs was 0.036 ± 0.005 mg. The NLG populations do not exhibit a significant difference in percent initial drug loaded ($p = 0.069$). Both NLG populations load similar amounts of AZT despite significant differences in lipid yield.

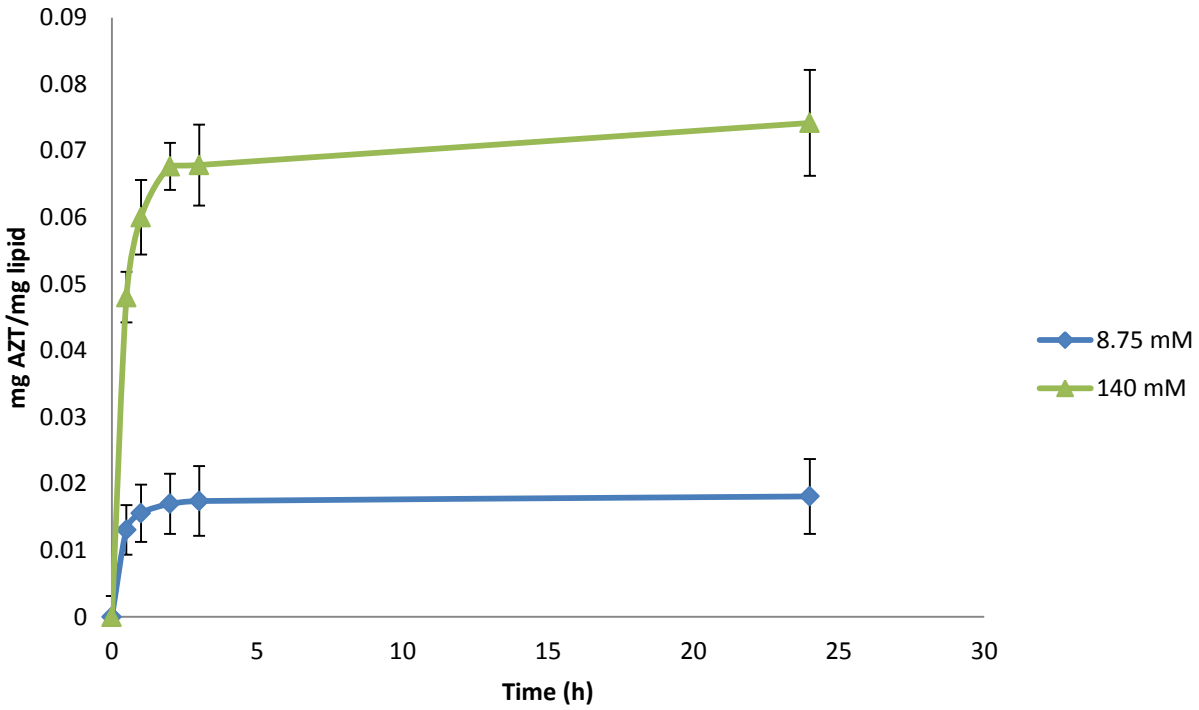

Figure 6: AZT release from variably crosslinked NLGs normalized to lipid recovery. High crosslink NLGs appear to release a greater amount of encapsulated AZT over time relative to lipid mass.

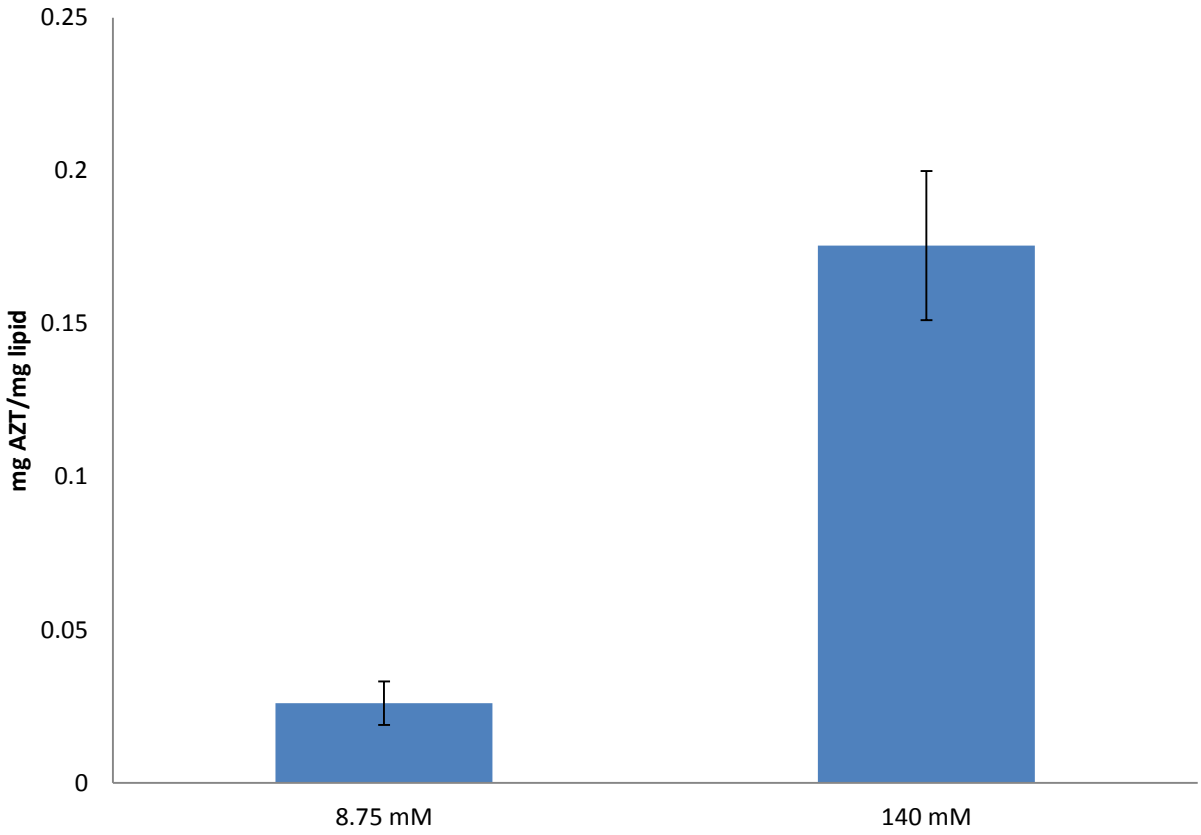

Figure 7: Drug loading in variably crosslinked NLGs normalized to lipid yield. The NLG populations load significantly different masses of AZT per mass lipid ($p = 0.005$) Lipid yield for 8.75 mM NLGs was 1.08 ± 0.27 mg, while lipid yield for 140 mM NLGs was 0.21 ± 0.04 mg. This indicates that high crosslink NLGs encapsulate more drug per particle than low crosslink NLGs.